ESTEEM Academic Journal
Vol. 13, June 2017, 18-29

NUMERICAL SIMULATION OF THE ELECTRIC FIELD GRADIENT SQUARED IN A NEW ELECTRODE CONFIGURATION FOR FOULING SUPPRESSION IN SUBMERGED MEMBRANE BIOREACTORS

Bouthaina Larbi[1], Alaa Alhawari[1], Fei Du[2], Michael Baune[2], and Jorg Thöming[2]

[1]*Department of Civil and Architectural Engineering, College of Engineering, Qatar University, 2713 Doha, Qatar*
[2]*Center of Environmental Research and Sustainable Technology, University of Bremen, Leobener Str., D 28359 Bremen, Germany*

**Corresponding author: bouthaina.larbi@qu.edu.qa*

ARTICLE HISTORY

Received
1 January 2017

Received in revised form
29 March 2017

Accepted
13 April 2017

ABSTRACT

Fouling is one of the central problems in submerged membrane bioreactors (MBRs), and the use of additional forces for anti-fouling has gained increasing attention in the recent years. In this study, a novel fouling suppression system in MBRs based on the application of AC dielectrophoresis force is proposed. The feasibility of the new system is demonstrated based on numerical simulations. To this end, the impact of electrode configuration (i.e. electrode geometry, the distance between electrodes, insulation properties & insulation thickness) on the DEP force i.e. on the electric field gradient squared (EFG), are studied for an optimal design of the new system. It was found that the EFG is high on the membrane surface when the electrode diameter and the distance between electrodes are smaller. Obtained results also showed a drop of the electric field gradient squared at the mid between two electrodes with highest EFG value on the electrode. Finally, numerical simulations revealed that a thickness of 20 µm of TiO_2 insulation is optimal to generate sufficient DEP force while avoiding joule heating problems.

Keywords: Dielectrophoresis; electric field gradient squared; interdigitated electrodes; activated sludge; MBRs

1. INTRODUCTION

Submerged membrane bioreactor (MBRs) is now the more common MBR configuration for wastewater treatment. It differs from conventional activated sludge system since a membrane module is used instead of the secondary clarifier to separate activated sludge from the final

p-ISSN 1675-7939; e-ISSN 2289-4934

effluent. In MBRs, the membrane separation is carried out with vacuum-driven membranes immersed directly into the bioreactor.

In comparison with the traditional sewage treatment techniques, MBRs presents many advantages such as fewer space requirements, lower energy consumption, higher quality of effluent, and easier handling (Xiang & Bo, 2001; Yin & Chen, 2001). Nevertheless, it also has some drawbacks, such as membrane fouling. This fouling problem is a major obstacle in diverse industrial and medical applications based on membrane separation process. It refers to membrane pore obstruction and sludge cake deposition which results in an unstable permeate flux or an increase of the transmembrane pressure depending on the operation mode. One of the proposed solutions to the fouling problem is the application of additional force. The inherent advantage of applying a force field is to prevent the formation of the fouling layer during the filtration process. By consequence, this solution avoids stopping the filtration operation to clean the membrane, which is the case in conventional methods: back-pulsing and flushing techniques. Some studies used a direct current (DC) electric field in a cross-flow membrane filtration process (Henry & Lawler, 1977; Lee & Gidaspow, 1980; Verdegan, 1986; Wakeman & Tarleton, 1987; Yukawa, 1983). These researches had focused more attention on using the electrophoretic (EP) effects to reduce fouling. In addition, this method is well adapted to reduce fouling problems associated with only charged particles and colloids (Wakeman & Tarleton, 1991). Because of the complexity of the feed suspensions, the use of this method is not possible in many cases (Kyllönen, Pirkonen, & Nyström, 2005). Moreover, the application of bare electrodes required by EP will result in an electrochemical reaction, resulting in pH modification or even the production of toxic by-products, and increase the risk of short circuit and human electric shock (Du, Baune, & Thöming, 2007). Du et al. (2013) and Du, Hawari, Baune and Thoming (2009) were one of the first to experimentally examine a lab scaled dielectrophoretic cross-flow membrane filtration process. A pulsed DEP intensified cross-flow membrane filtration process with an applied AC electric field, and 200 kHz was considered. They found that the working time for the membrane to have 50% permeate flux of the initial flux is more than three times longer. With this DEP based method, nearly all the particles in suspension can be prevented from depositing on the membrane regardless of the particles being charged or uncharged. Moreover, the DEP force is found to be more dependent upon the electric field gradient than the voltage applied. When the applied voltages in DEP and EP systems are identical, the dielectrophoretic motion of particle presents much higher speed than electrophoretic movement (Thoming, Du, & Baune, 2006). However, during the experiments Joule heating occurred which increased the temperature in the MBR tank. Thus, this can affect both membrane pore size and biomass.

In the present study, an optimized new electrode configuration for the case of MBRs is proposed. This system is based on the application of alternating current (AC) dielectrophoresis (DEP) force in an inhomogeneous electrical field. The new configuration is designed with the aim of generating sufficient DEP force able to push particles away from the membranes while preventing Joule heating effect. Its feasibility is demonstrated based on numerical simulation of the electric field gradient squared (EFG). To this end, the influence of electrodes configuration parameters (i.e. electrode geometry, the distance between electrodes, insulation properties & insulation thickness) on the EFG is studied for an optimal design of the new system.

p-ISSN 1675-7939; e-ISSN 2289-4934

2. DIELECTROPHORESIS

Dielectrophoresis was first defined by Pohl (Pohl, Pollock, & Crane, 1978) as the motion of neutral particle caused by dielectric polarization in an inhomogeneous electric field. With the polarization of particle in an electric field, a dipole moment is induced in the particle and can be expressed as two equal but opposite charges at the particle boundary. However, when the charges are not uniformly distributed on the particle surface, a macroscopic dipole will be created. If the electric field is inhomogeneous, the local electric field and resulting force on both sides of the particle are different, and then a net force arises termed as dielectrophoretic force FDEP. For a homogeneous sphere of radius 'a' in a medium with permittivity εm, the DEP force can be calculated as shown in Equation (1):

$$F_{DEP} = 2\pi a^3 \varepsilon_0 \varepsilon_m Re(\tilde{K}) \nabla |E|^2 \quad (1)$$

Where Re($\tilde{K}$), is the real part of the Clausius-Mossotti ($\tilde{K}$) factor, ε_0 is the permittivity of free space with the value of 8.854×10^{-12} F/m and ε_m is the permittivity of the medium. The Clausius-Mossotti factor describes the frequency dependence of the effective dielectric polarizability of the particle in suspension as shown by Equation (2).

$$\tilde{K} = \frac{\tilde{\varepsilon}_p - \tilde{\varepsilon}_m}{\tilde{\varepsilon}_p + 2\tilde{\varepsilon}_m} \quad (2)$$

Where, $\tilde{\varepsilon}_p$ and $\tilde{\varepsilon}_m$, are complex permittivity of the particle and the suspension medium respectively. The calculation of the complex permittivity ($\tilde{\varepsilon}$) is given as:

$$\tilde{\varepsilon} = \varepsilon - \frac{j\sigma}{\omega} \quad (3)$$

ε is the dielectric constant and σ (S/m) is the conductivity,ω (rad/s) is the angular frequency of the applied electric field $\omega = 2\pi f$ in which f (Hz) is the frequency, and j =$\sqrt{-1}$.

The direction of particle movement depends on the sign of the Clausius-Mossotti factor $\tilde{K}$, which in turn depends on the frequency. In a certain electric field, with a certain frequency, when the permittivity of particle is higher than that of suspending medium, the direction of dielectrophortic force of the particle is along the direction of electric field gradient, which directs from lower electric field to higher electric field. In this case, the particle is towards higher electric field region, presenting positive DEP effect (pDEP). Inversely, when the real part of Clausius-Mossotti factor is negative, i.e. the permittivity of particle is lower than that of the suspending medium, the dielectrophortic force directs oppositely to the direction of electric field gradient, which is from higher electric field to lower electric field. Therefore, the dielectrophoretic force can move the particle towards the lower electric field region, presenting negative DEP effect (nDEP). In the case of this study, it is expected that the biomass particles will be affected by a negative DEP because their permittivity is lower than that of the surrounding medium.

3. DESIGN OF THE DEP SYSTEM

The proposed DEP submerged MBR membrane module is composed of two membranes, two spacers, two ABS frames with cylindrical electrodes integrated into the two frames (Figure 1).

p-ISSN 1675-7939; e-ISSN 2289-4934

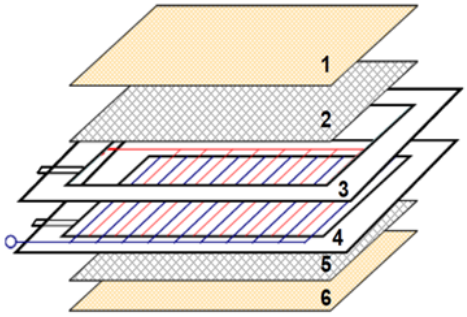

Figure 1: The proposed DEP submerged MBR membrane module. 1 & 6 are flat sheet membranes; 2 & 5 are two plastic spacers; 3 & 4 are two ABS frames with electrodes integrated into the frames)

The two frames of the membrane module are processed with channels for integrating electrodes. The two spacers are put on the two frames for supporting the membranes and enhancing the permeate flux out of the membrane module. The microfiltration membranes are welded onto the frames. At one end of the membrane module, two leads are for electric connection and one opening is designed for the output of permeate flow. The electrodes are interdigitatedly installed (IDE).

4. NUMERICAL METHOD AND MATERIAL PROPERTIES

The objective of the simulation study is to identify the optimal electrode configuration design for fouling reduction while avoiding Joule heating effect within the system. The governing equations are those of the coupling of the electric and heat transport phenomena that typically take place in DEP systems.

4.1 Governing equations

4.1.1 Electric field

The electric field E within the fluid is governed by the current conservation equation. For absence of any external sources of charge and current, the equation can be expressed as in the following formula (4):

$$\nabla.\left(\sigma E + \frac{\partial D}{\partial t}\right) = 0 \; and \; E = -\nabla V \tag{4}$$

Where $D = \varepsilon E$ is the electric field displacement, t is the time coordinate, and V is the electric potential. The electric field is restricted only to the fluid domain by electrically insulating the reactor walls. Electrodes are imposed alternately with the applied voltage V_0 (RMS) and zero voltage (i.e. grounded). The initial value of the electric potential is zero everywhere within the fluid.

p-ISSN 1675-7939; e-ISSN 2289-4934

4.1.2 Temperature field

The application of electric field leads to Joule heating within the fluid and increase the temperature (T) gradients that spread across the fluid with time. The transport of heat is governed by the energy equation (5):

$$\rho C_p \left(\frac{\partial T}{\partial t} + u.\nabla T\right) = k\nabla^2 T + \sigma E^2 \quad (5)$$

Where $\rho, C_{p,}$ *and* k are the fluid density, specific heat capacity of the fluid, and thermal conductivity of the fluid, and u is the fluid velocity. σE^2 represents the time averaged Joule heating, which exists only in the fluid domain. The initial temperature of the whole system is set to room temperature. In the case of this study, no flow is imposed which permits the design of the system based on the worst case.

4.1.3 Computational domain and boundary conditions

The computational domain presents a two-dimensional model of the proposed IDE configuration as shown in Figure 2. It includes the insulated electrodes cross sections floating in a fluid with conductivity equal to 0.05 S/m. This two-dimensional model could provide the necessary predictions regarding the established electric field gradient squared and the temperature gradient within the fluid and on the membrane surface. A characteristic length of the electrodes (10 cm) was considered by the "out of the plane thickness" settings when solving the coupled electric and heat transfer equations.

The following boundary conditions were imposed: $V=V_0$ and V=0 (i.e. grounded) applied interdigitatedly on the electrodes.

The walls of the reactor are electrically ($n.(\sigma\nabla V) = 0$) and thermally insulated ($n.q = 0$), q is the heat flux, and n is the unit normal vector.

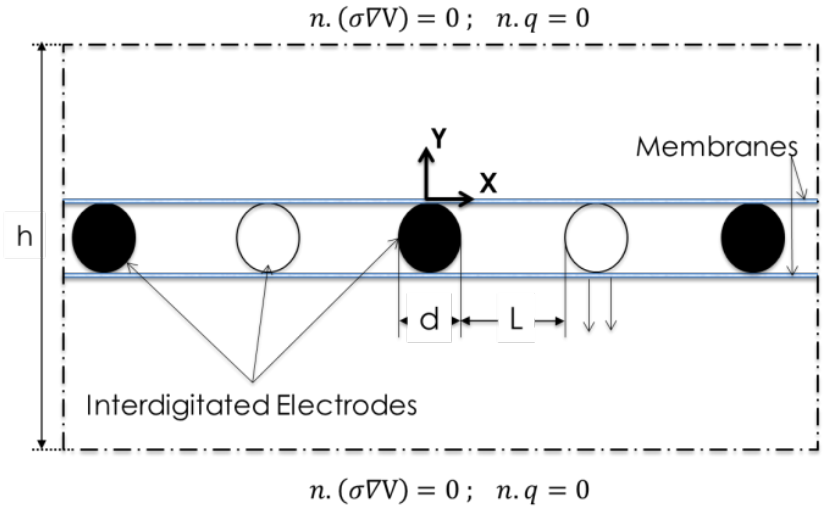

Figure 2: The two-dimensional model for the IDE configuration

p-ISSN 1675-7939; e-ISSN 2289-4934

4.1.4 Numerical method and materials properties

Numerical simulations were performed using Comsol Multiphysics 5.2, commercial finite element simulation software. The "Joule Heating" Multiphysics coupling in the software was used. It couples "electric current" and "heat transfer" interfaces. The two-dimensional geometry was performed using the drawing tools in COMSOL. The diameter of cylindrical electrodes was designed to be 2 mm. The distance from the edge to edge of the electrodes varied from 2 mm to 8 mm. The thickness of insulation material ranges from 2 µm to 80 µm. Two insulation materials are examined: titanium dioxide TiO2 and aluminum oxide Al_2O_3. The geometry was then meshed with triangular meshes. The insulation layer consists of fine mesh elements than the rest of the domain due to their small dimension. The temperature was the coupling variable in solving heat and electric equations as it affects the fluid properties. Therefore, the temperature dependence of fluid permittivity and conductivity was considered using the expressions (6) and (7):

$$\varepsilon(\mathrm{T}) = \varepsilon_0[1 + \alpha(T - T_0)] \quad (6)$$

$$\sigma(\mathrm{T}) = \sigma_0[1 + \beta(T - T_0)] \quad (7)$$

Where σ_0 is the electric conductivity of the fluid at the initial temperature and β is the linear temperature coefficient. The values of the constants and material properties used in the numerical simulation are listed in Table1.

5. RESULTS

The coupling of the electric and the heat phenomenon in the IDE-DEP configuration was studied. A reference case of 250 V - 100 kHz was considered for all the simulations. The figures from 3 to 6 show the simulated electric field gradient squared $\nabla|E|^2$ as opposed to the positions on the surface of the membrane (x-coordinate). Independently of the variables and the parameters of the study, a uniform distribution was found in all the simulations of the EFG. This distribution presented a drop of the EFG at the midway between two electrodes and the highest one on the electrode (Figure 3). It is expected that this distribution will allow enhancing the DEP fouling suppression by removing the particles agglomerate adhered to the membrane at lower electric field regions (Du et al., 2009).

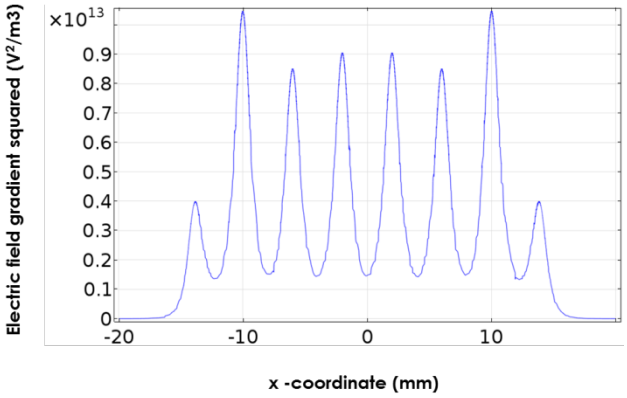

Figure 3 : Electric field gradient squared distribution along the feed flow direction. Simulations performed with 8 electrodes, medium conductivity 0.05 S/m, d: L =2:2, 2 µm TiO2 insulation

p-ISSN 1675-7939; e-ISSN 2289-4934

Table 1: The values of the constants and material properties used in the numerical simulation

Symbol	Value	Unit	Description
T_0	293	K	Room temperature
ε_0	80	F/m	Fluid permittivity at T_0
σ_0	0.05	S/m	Fluid Electrical conductivity
ρ	1000	Kg/m^3	Fluid density
$\sigma_{(TiO2)}$	$10E^{-4}$	S/m	Electrical conductivity of TiO_2
$\varepsilon_{(TiO2)}$	86	1	Relative permittivity of TiO_2
$\sigma_{(Al2O3)}$	$10E^{-12}$	S/m	Electrical conductivity of Al_2O_3
$\rho_{(Al2O3)}$	3965	kg/m3	Density of Al_2O_3
$\varepsilon_{0(Al2O3)}$	5.7	1	Relative permittivity of Al_2O_3
$C_{p(Al2O3)}$	730	J/(kg.K)	Heat capacity at constant pressure of Al_2O_3
$K_{(Al2O3)}$	35	W/(m.K)	Thermal conductivity of Al_2O_3
$\alpha_{(Al2O3)}$	$6.5.10E^{-6}$	1/K	Coefficient of thermal expansion of Al_2O_3
$\sigma_{(Stainless\ steel)}$	$1.74.\ 10E^{6}$	S/m	Electrical conductivity of stainless steel
$\rho_{(Stainless\ steel)}$	7800	kg/m3	Density of stainless steel
$\varepsilon_{0(Stainless\ steel)}$	1	1	Relative permittivity of stainless steel
$C_{p(Stainless\ steel)}$	460	J/(kg.K)	Heat capacity at constant pressure of stainless steel
$K_{(Stainless\ steel)}$	27	W/(m.K)	Thermal conductivity of stainless steel

5.1 Impact of electrode configuration on the electric field gradient squared

As it was mentioned before, the electrodes diameter d was equal to 2 mm in all the simulations. Then, the EFG was simulated for different distance L between electrodes from 2 to 8 mm. Results of these simulations (Figure 4) showed much higher EFG when the distance between electrodes was smaller for the same electrodes diameter and same insulation material (TiO2) and thickness (2 µm). Numerical results also showed that the use of thinner insulation film of TiO2 led to a higher EFG (Figure 5).

p-ISSN 1675-7939; e-ISSN 2289-4934

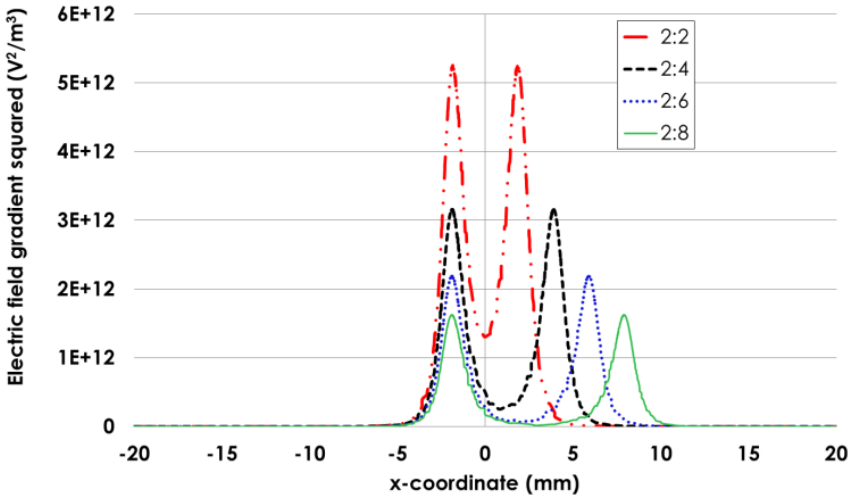

Figure 4: Impact of the distance between electrodes on the EFG. Simulations performed with 2 electrodes, medium conductivity of 0.05 S/m, d: L = [2:2, 2:4, 2:6, 2:8], 2 µm TiO_2 insulation, 250 V

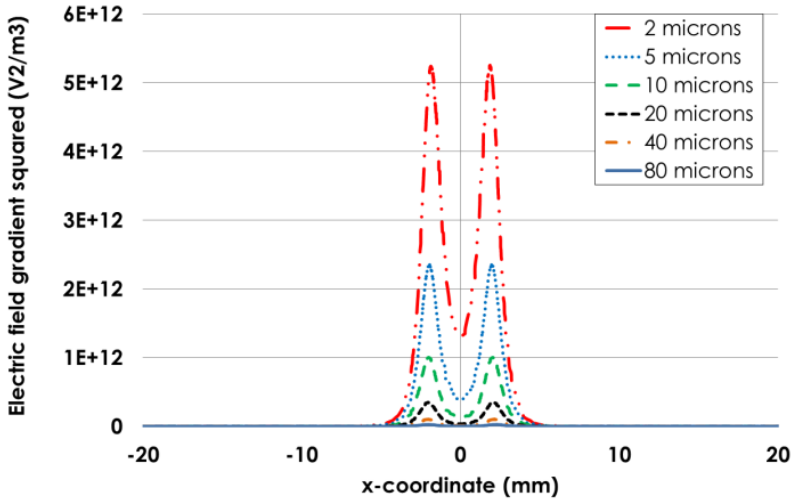

Figure 5: Effect of insulation thickness on the EFG. Simulations performed with 2 electrodes, medium conductivity 0.05 S/m, d: L= 2:2, 2 µm TiO2 insulation, 250 V

Al_2O_3 insulation material was tested, the obtained EFG was considerably lower than the one obtained when using TiO_2 under the same conditions (fluid conductivity, voltage input, electrodes configuration). Therefore, a higher EFG could be obtained when using a thin insulation layer of TiO_2 while keeping a small distance between electrodes.

5.2 Side effects: Joule heating and high pass filter effect

5.2.1 Joule heating

With aqueous medium, two side effects often occur in DEP systems, high pass filter, and Joule heating effect. The study of the temperature field in the fluid showed that although a

p-ISSN 1675-7939; e-ISSN 2289-4934

higher EFG was recorded when the distance between electrodes and the thickness of insulation film was small, the temperature gradient in the fluid increases within these conditions. It was found that with an effective control of the electric field properties, the influence of Joule heating could be alleviated (Figure 6).

(a)

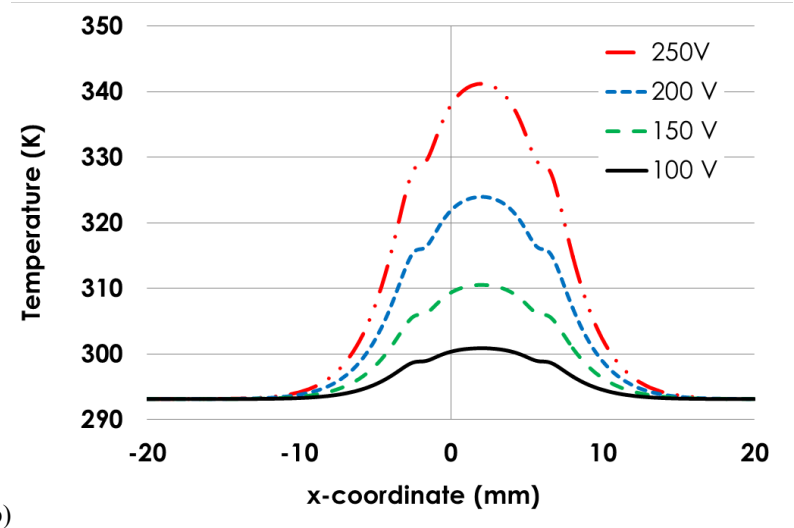

(b)

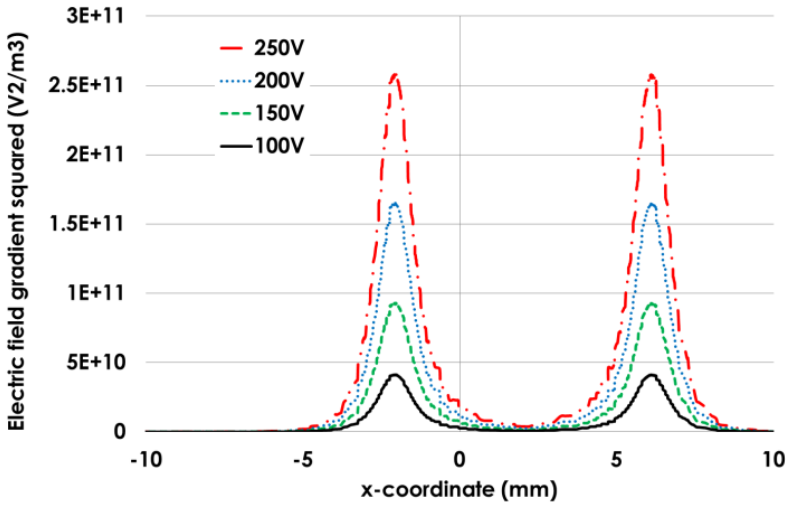

Figure 6: Impact of voltage input on reducing temperature gradient within the fluid 1 mn after applying the electric potential (a). The impact of the voltage input on the EFG (b). Simulations performed with 2 electrodes, medium conductivity 0.05 S/m, d: L= 2:6, 20 µm TiO2 insulation

5.2.2 High pass filter effect

Electrodes should be insulated to avoid any of these problems which include human electric shock, side chemical reactions and a short circuit. However, this insulation will reduce the efficiency of DEP in low frequencies and will increase the amount of consumed energy in the system because the insulated electrodes together with the conductive aqueous medium will

p-ISSN 1675-7939; e-ISSN 2289-4934

generate a high pass filter effect (Baune, Du, & Thoming, 2008). Baune et al. (2008) simulated the influence of properties of insulation film on the high-pass-filter effect, and demonstrated that a properly thin insulation film with high permittivity will reduce the influence of high-pass filter effect (Baune et al., 2008). However, a thin insulation thickness leads to high-temperature gradient within the fluid. Therefore, an optimal choice of electrodes geometrical parameters and the applied voltage should be identified to avoid the opposed side effects: the joule heating and the high pass filter effect. In this study, the voltage fraction for electrode configuration with 20 µm insulation thickness was simulated as shown in Figure 7.

The fraction of voltage was found to be around 98% at a frequency of 200 kHz with an aspect ratio of 2:6. Under these conditions (2:6, 20 µm, 200V), the value of the EFG obtained by COMSOL simulations is about 1.6 $\times 10^{11}$ V^2/m^3 (Figure 6b). The calculation of the Stokes' drag force for a spherical particle of 5 µm diameter swimming in the water with a speed of 2 $\times 10^{-8}$ m/s, show that the minimum required EFG to push this particle is about 2.5×10^{10} V^2/m^3. The bioparticles sizes range from 0.1 µm to 15 µm [16].

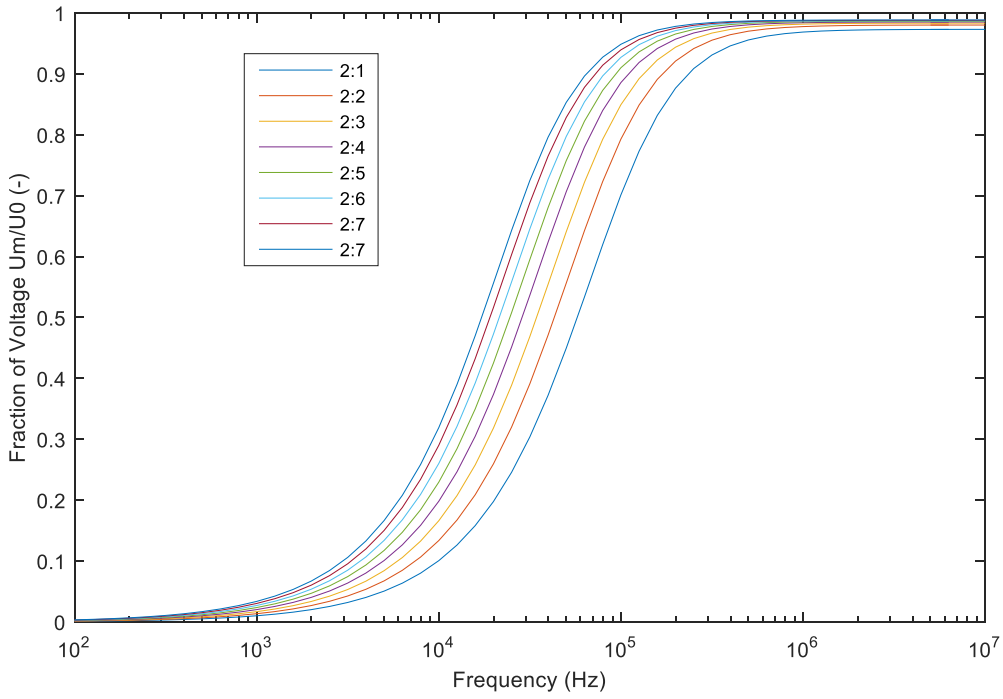

Figure 7: Frequency dependence of voltage fraction for different aspect ratios (d:L). V_0 is the applied voltage (= 200 V), V_m voltage across medium among electrode configurations. Aqueous medium with the conductivity of 0.05 S/m; IDE insulated by 20 µm of TiO_2.

The simulation of temperature within the fluid under these conditions gives a rise of 10%. It is important to note that the simulated system is a closed system where no circulation of fluid occurred. In practice, an open system with a circulation of cool water will be considered which could alleviate more the Joule heating effect. Moreover, a pulsation of the applied electric field is planned to control the temperature rise and then reduce the energy consumption.

p-ISSN 1675-7939; e-ISSN 2289-4934

6. CONCLUSION

In this work, a novel electrode configuration for fouling suppression system based on the application of AC dielectrophoresis force is proposed. The feasibility of the new configuration is demonstrated based on numerical simulations of the electric field gradient squared. A parametric study is accomplished with the consideration of the side effects for an optimal design of the configuration. It was found that a configuration of 2:6 mm, 20 μm TiO2 insulation thickness, 200 V voltage input and 200 kHz could present a balance to get effective DEP force for fouling suppression while avoiding Joule heating effect. Experimental tests are still necessary to confirm these numerical findings.

7. ACKNOWLEDGMENT

This research is made possible by NPRP award (NPRP 7-089-2-044) from Qatar National Research Fund (QNRF).

REFERENCES

Baune, M., Du, F., & Thoming, J. (2008). Dielectrophoresis-Bridging the scale in modeling and application. *P.J. Plath, E. Hass (Eds.), Vernetzte Wissenschaften, Logos Verlag Berlin GmbH, Berlin*, 47–64.

Du, F., Baune, M., & Thöming, J. (2007). Insulator-based dielectrophoresis in viscous media—Simulation of particle and droplet velocity. *Journal of Electrostatics*, *65*(7), 452–458. http://doi.org/10.1016/j.elstat.2006.10.010

Du, F., Ciaciuch, P., Bohlen, S., Wang, Y., Baune, M., & Thöming, J. (2013). Intensification of cross-flow membrane filtration using dielectrophoresis with a novel electrode configuration. *Journal of Membrane Science*, *448*(JANUARY), 256–261. http://doi.org/10.1016/j.memsci.2013.08.016

Du, F., Hawari, A., Baune, M., & Thoming, J. (2009). Dielectrophoretically intensified cross-flow membrane filtration. *Journal of Membrane Science*, *336*(1–2), 71–78. http://doi.org/10.1016/j.memsci.2009.03.010

Henry, J.D.J. & Lawler, L. F. (1977). A solid/ liquid separation process based on cross flow and electrofiltration. . *AIChE Journal*, *23*(6), 851–859.

Kyllönen, H. M., Pirkonen, P., & Nyström, M. (2005). Membrane filtration enhanced by ultrasound: A review. *Desalination*, *181*(1–3), 319–335. http://doi.org/10.1016/j.desal.2005.06.003

Lee C., H., & Gidaspow, D. (1980). Crossflow Electrofilter for non-aqueous slurries. *Industrial & Engineering Chemistry Fundamentals.*, *19*(2), 166–175.

Pohl, H. A., Pollock, K., & Crane, J. S. (1978). Dielectrophoretic force: A comparison of theory and experiment. *Journal of Biological Physics*, *6*(3–4), 133–160. http://doi.org/10.1007/BF02328936

Thoming, J., Du, F., & Baune, M. (2006). Dielectrophoretic separation of oil-water-solid

p-ISSN 1675-7939; e-ISSN 2289-4934

dispersions–Selectivity and particle velocity.. *Fresenius Environ. Bull.*, *15*(7), 687–691.

Verdegan B. M. . (1986). Cross flow electrofiltration of petroleum oils.. *Separation Science and Technology*, *21*(6–7), 603–623.

Wakeman R. J. & E. S. Tarleton. (1987). Membrane fouling prevention in crossflow microfiltration by hte use of electric-fields. *Chemical Engineering Science*, *42*(4), 829–842.

Wakeman R. J. & E. S. Tarleton. (1991). An experimental study of electroacoustic crossflow microfiltration. *Chemical Engineering Research and Design: Transactions of the Institution of Chemical Engineers.* , *69*(Part A), 386–397.

Xiang, Z., & Bo, F. (2001). Optimization of the Operation Parameters on MBR and Membrane Fouling Control. *Water & Wastewater Engineering*.

Yin J., & Chen Y. Xu. (2001). Membrane fouling in membrane bioreactors. *Tech. Equip. Environ. Pollut. Control* , *2*((3)), 62–68.

Yukawa, H., Shimura, K., Suda, A., & Maniwa, A. (1983). Cross flow electro-ultrafiltration for colloidal solution of protein. *Journal of chemical engineering of Japan*, *16*(4), 305-311.

p-ISSN 1675-7939; e-ISSN 2289-4934